

# Glass formation in the multicomponent chalcogenide GeSe<sub>2</sub>-Sb<sub>2</sub>Se<sub>3</sub>-PbTe system

V. VASSILEV\*, M. RADONOVA, S. BOYCHEVA<sup>a</sup>, E. FIDANCEVSKA<sup>b</sup>

*University of Chemical Technology and Metallurgy, Department of Non-Ferrous Metals and Semiconductor Technologies – Sofia, 8 Kl. Ohridsky Blvd., 1756 Sofia, Bulgaria*

<sup>a</sup>*Technical University –Sofia, Department of Thermal and Nuclear Power Engineering, 8 Kl. Ohridsky Blvd., 1000 Sofia, Bulgaria*

<sup>b</sup>*University „St. Cyril and Methodius“, Faculty of Technology and Metallurgy, Rudjer Boskovic 16, 1000 Skopje, Macedonia*

New chalcogenide glasses (ChGs) from the GeSe<sub>2</sub>-Sb<sub>2</sub>Se<sub>3</sub>-PbTe system were synthesized. The glass-forming region was determined by the help of visual and X-ray diffraction analyses. It is situated in the GeSe<sub>2</sub>-rich part in the Gibbs' diagram and partially lies on the GeSe<sub>2</sub>-Sb<sub>2</sub>Se<sub>3</sub> (0–70 mol% Sb<sub>2</sub>Se<sub>3</sub>) and GeSe<sub>2</sub>-PbTe (15.0–57.5 mol% PbTe) sides. No glasses were obtained in the binary Sb<sub>2</sub>Se<sub>3</sub>-PbTe system. The ChGs were investigated with respect to their phase transformations temperatures (glass transition T<sub>g</sub>, crystallization T<sub>cr</sub> and melting T<sub>m</sub>) and density (d). The compactness (C) and Hruby's criterion (K<sub>G</sub>) were calculated from the measured values for the thermal and mechanical characteristics.

(Received July 06, 2009; accepted July 20, 2009)

*Keywords:* Chalcogenide glasses, Physicochemical properties, Thermomechanical characteristics

## 1. Introduction

Recently, the chalcogenide glasses (ChGs) attract much scientific attention as advanced materials due to the unique combination of their properties: excellent chemical stability in aggressive environments, relatively high ion conductivity, transparency in the near and far infrared region, low optical losses and high refraction coefficient, very good protective properties, etc. [1,2]. Meanwhile, thermo-, electro- and photo-stimulated reversible structural transformations of the glass↔crystal type have been observed in ChGs [3,4]. Moreover, the compositional and structural diversity of the multicomponent ChGs allow widely the properties in a wide range and this recommend them for a large variety of applications. The ChGs are successfully applied in optical fibers and waveguides, functional components in the integral optoelectronics, discrete electronic components and high-speed switches, information recording media [5,6], functional materials for ion-selective electrodes [7,8] and chemical sensors for registration of noxious contaminations in gaseous and liquid media [9-12].

The glasses from the Ge-Se system and those based on the GeSe<sub>2</sub> glass-former have been intensively studied as glassy matrices for different additives because of their high glass-forming ability and aging resistance [13]. The basic structural units in the glasses of this sub-group are Se-chains and GeSe<sub>4/2</sub>-tetrahedrons, which can be combined each other in different manners in every particular system. On the other hand, it is well known that Sb<sub>2</sub>Se<sub>3</sub> added to GeSe<sub>2</sub> improves the GeSe<sub>2</sub> glass-forming ability and extends the glass formation limits [14,15].

The present research is directed to the preparation of novel multicomponent ChGs from the GeSe<sub>2</sub>-Sb<sub>2</sub>Se<sub>3</sub>-PbTe system, determination of the glass-forming region and investigation of the main physicochemical properties of the obtained glasses. Taking into account our previous observation from the studies on pseudo-ternary chalcogenide and chalcohalide systems, we could expect that adding PbTe to the binary GeSe<sub>2</sub>-Sb<sub>2</sub>Se<sub>3</sub> system, glasses in a wide concentration range will be obtained with appropriate properties for application in ion-selective membrane electrodes, gas sensors and IR-optic devices.

## 2. Experimental procedures

The glass-forming region in the GeSe<sub>2</sub>-Sb<sub>2</sub>Se<sub>3</sub>-PbTe system was determined by the help of 27 synthesized compositions. The starting compounds GeSe<sub>2</sub>, Sb<sub>2</sub>Se<sub>3</sub> and PbTe were prepared from the corresponding elements Ge, Se and Te with 5N of purity and Sb and Pb - 4N. The initial compound GeSe<sub>2</sub>, Sb<sub>2</sub>Se<sub>3</sub> and PbTe and the samples from the GeSe<sub>2</sub>-Sb<sub>2</sub>Se<sub>3</sub>-PbTe system were produced by direct mono-temperature synthesis in quartz ampoules evacuated to residual pressure of 0.133 Pa and sealed. The syntheses were performed with step-wise heating up to 500, 800 and 950 °C, at rates 3-4, 2-3 and 2-3°C min<sup>-1</sup>, respectively. Homogenizing annealing of the melts were carried out at these temperatures for 0.5, 0.5 and 2.0 h, correspondingly, combined with continuous vibration stirring at the highest temperature. The syntheses were ended by cooling of the melts in a mixture of water and ice.

The synthesized samples were subjected to visual and X-ray diffraction analyses (XRD). XRD was performed by X-ray equipment TUR-M61 with  $\text{CuK}\alpha$ -radiation and Ni-filter,  $\theta=5$ -40.

Phase transformations temperatures of the ChGs - glass transition  $T_g$ , crystallization  $T_{cr}$  and melting  $T_m$  were determined by differential thermal analysis (DTA) using measuring set-up F.Paulik-J.Paulik-L.Erdey, MOM-Hungary. DTA was carried out as the glassy samples in quantity of 0.3 g were heated at rate 10 °C/min in evacuated and sealed Stepanov's vessels. Calculated  $\gamma\text{-Al}_2\text{O}_3$  was used as a reference substance. The density ( $d$ ) was measured by a hydrostatic method in toluene.

### 3. Results

The compositions of the synthesized samples from the  $(\text{GeSe}_2)_x(\text{Sb}_2\text{Se}_3)_y(\text{PbTe})_z$  systems, where  $x+y+z=100$  mol %, are listed in Table 1. The obtained samples were subjected to visual and X-ray diffraction analyses and their state was defined as amorphous, crystalline or amorphous+crystalline. The glasses from the  $\text{GeSe}_2\text{-Sb}_2\text{Se}_3\text{-PbTe}$  system are dark colored with a strong luster and typical for the glassy state conchoidal fracture when the sample is broken.

Table 1. Composition and state of the synthesized samples from the  $\text{GeSe}_2\text{-Sb}_2\text{Se}_3\text{-PbTe}$  system.

№	Composition, mol %			State	№	Composition, mol %			State
	$\text{GeSe}_2$	$\text{Sb}_2\text{Se}_3$	$\text{PbTe}$			$\text{GeSe}_2$	$\text{Sb}_2\text{Se}_3$	$\text{PbTe}$	
1	81	9	10	glass	15	32.5	32.5	35	crystal
2	54	36	10	glass	16	90	0	10	crystal
3	36	54	10	glass	17	45	5	50	glass
4	27	63	10	crystal	18	48	12	40	glass
5	40.5	4.5	55	glass+crystal	19	26.2	48.8	25	crystal
6	32	48	20	glass	20	38.5	16.5	45	glass
7	31.5	58.5	10	glass	21	63	7	30	glass
8	24	56	20	crystal	22	56	14	30	glass
9	28	42	30	crystal	23	42	28	30	glass
10	36	24	40	glass+crystal	24	35	20	45	crystal
11	40	10	50	glass+crystal	25	35	15	50	crystal
12	72	18	10	glass	26	90	5	5	glass
13	28	52	20	glass	27	30	45	25	glass
14	35	35	30	glass+crystal					

Typical X-ray diffractograms of the examined samples are plotted in Fig. 1. The performed XRD analysis shows that the compositions located in the glass-forming region possess the typical for the amorphous state diffractograms; they are characterized by X-ray amorphous plateau and absence of diffraction peaks (Fig. 1 (1)). The compositions outlining the glass-formation boundaries are characterized by diffractograms considerably richer in diffraction reflexes although of lower intensity (Fig. 1 (2)), while for the compositions located out of the glass-forming region the diffraction pattern is typical for the crystalline state with much more intense well-expressed peaks (Fig. 1 (3)).

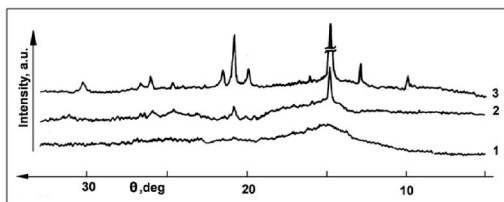


Fig. 1. Roentgenogram of samples of the  $\text{GeSe}_2\text{-Sb}_2\text{Se}_3\text{-PbTe}$  system: (1)  $(\text{GeSe}_2)_{42}(\text{Sb}_2\text{Se}_3)_{28}(\text{PbTe})_{30}$ ; (2)  $(\text{GeSe}_2)_{40}(\text{Sb}_2\text{Se}_3)_{10}(\text{PbTe})_{50}$ ; (3)  $(\text{GeSe}_2)_{35}(\text{Sb}_2\text{Se}_3)_{15}(\text{PbTe})_{50}$ .

The determined state of the all studied compositions from the  $\text{GeSe}_2\text{-Sb}_2\text{Se}_3\text{-PbTe}$  system is pointed in Table 1.

The schematic diagram of the X-ray diffraction spectra for some investigated samples is presented in Fig. 2. Evidently, the reflections of the initial compounds appear depending on the alloy compositions, as predominantly crystallize  $\text{Sb}_2\text{Se}_3$  and  $\text{PbTe}$  phases. For the compositions (p.4 and p.25) falling out of the glass-forming region intensive reflexes with considerable quantity were registered. At the compositions enriched in  $\text{PbTe}$  mainly the  $\text{PbTe}$  lines present, while at those with higher  $\text{Sb}_2\text{Se}_3$  content - its lines prevail. For the compositions outlining the glass formation boundaries, the reflexes of the crystal phases  $\text{PbTe}$  and  $\text{Sb}_2\text{Se}_3$  restricted in number because the quantity the amorphous phase prevails. Particularly interesting in this case is that no lines of  $\text{GeSe}_2$  or eventually of  $\text{GeSe}$  and  $\text{Se}$  were registered, which almost ever appear at the  $\text{GeSe}_2$ -based alloys [16].

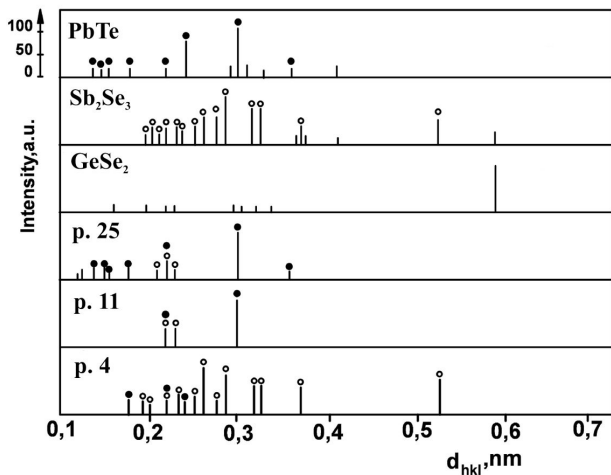


Fig. 2. Schematic X-ray diagram of samples from the investigated system: p.4 –  $(\text{GeSe}_2)_{27}(\text{Sb}_2\text{Se}_3)_{63}(\text{PbTe})_{10}$ ; p.11 –  $(\text{GeSe}_2)_{40}(\text{Sb}_2\text{Se}_3)_{10}(\text{PbTe})_{50}$ ; p.25 –  $(\text{GeSe}_2)_{35}(\text{Sb}_2\text{Se}_3)_{15}(\text{PbTe})_{50}$ ; 4 –  $\text{GeSe}_2$  [17]; 5 –  $\text{Sb}_2\text{Se}_3$  [18]; 6 –  $\text{PbTe}$  [19].

On the basis of the performed synthesis and the results obtained by the visual and X-ray diffraction analyses, the glass-forming region in the  $\text{GeSe}_2\text{-Sb}_2\text{Se}_3\text{-PbTe}$  system was defined – Fig. 3. It is situated in the  $\text{GeSe}_2$ -rich part in the Gibbs' diagram and partially lies on the  $\text{GeSe}_2\text{-Sb}_2\text{Se}_3$  (0–70 mol%  $\text{Sb}_2\text{Se}_3$ ) and  $\text{GeSe}_2\text{-PbTe}$  (15.0–57.5 mol%  $\text{PbTe}$ ) sides. No glasses were obtained in the binary  $\text{Sb}_2\text{Se}_3\text{-PbTe}$  system.

Typical DTA thermograms of ChGs from the investigated system are plotted in Fig. 4. They were used for determination of the characteristic temperatures:  $T_g$ ,  $T_{cr}$  and  $T_m$ , which are summarized in Table 2.

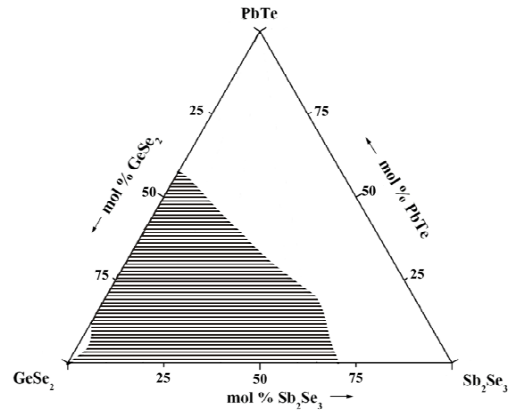


Fig. 3. Glass-forming region in the three-component  $\text{GeSe}_2\text{-Sb}_2\text{Se}_3\text{-PbTe}$  system.

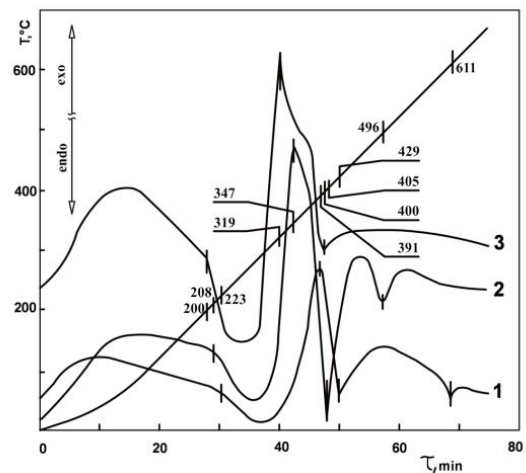


Fig. 4. Thermograms of ChGs from the  $\text{GeSe}_2\text{-Sb}_2\text{Se}_3\text{-PbTe}$  system 1-sample 1; 2–sample 21; 3-sample 18 (see Table 2).

Table 2. Physicochemical properties of  $(\text{GeSe}_2)_x(\text{Sb}_2\text{Se}_3)_y(\text{PbTe})_z$  ChGs, where  $x+y+z=100$  mol %,  $m=y/(x+y)$ .

№	Composition, mol %			m	$T_g$ , °C	$T'_{cr}$ , °C	$T''_{cr}$ , °C	$T'_m$ , °C	$T''_m$ , °C	$K'_G$	d, $\text{g cm}^{-3}$	C
	x	y	z									
1	81	9	10	0.1	223	-	391	429	611	4.42	4.42	- 0.084
2	72	18	10	0.2	228	-	386	424	544	4.16	4.55	- 0.089
3	54	36	10	0.4	211	-	376	424	-	3.44	4.80	- 0.093
4	36	54	10	0.6	203	290	347	415	482	2.12	4.90	- 0.115
5	31.5	58.5	10	0.65	199	268	345	410	501	2.25	5.00	- 0.106
6	63	7	30	0.1	208	-	347	405	496	2.40	5.20	- 0.040
7	56	14	30	0.2	213	-	343	405	-	2.10	5.35	- 0.030
8	42	28	30	0.4	189	295	319	405	439	1.51	5.40	- 0.060
9	48	12	40	0.2	200	-	319	400	-	1.47	5.70	- 0.020
10	45	5	50	0.1	194	-	333	405	-	1.93	6.00	- 0.010

The measured values for density (d) of the investigated glasses are listed in Table 2.

Hruby's criterion  $K'_G$  and the compactness C were calculated by equations (1 and 2) [14]:

$$K_G = \frac{T_{cr} - T_g}{T_m - T_{cr}} \quad (1)$$

$$C = d \left\{ \sum_i \frac{M_i x_i}{d_i} - \sum_i \frac{M_i x_i}{d} \right\} \left[ \sum_i M_i x_i \right]^{-1} \quad (2)$$

where  $T_g$ ,  $T_{cr}$  and  $T_m$  are the temperatures of glass-transition, crystallization and melting, correspondingly;  $M_i$  and  $x_i$  are the molar mass and the molar fraction of the  $i$ -th component.

The dependences of  $T_{cr}$ ,  $T_m$ ,  $K_G$  and  $C$  from the composition of the ChGs expressed with the compositional ratio  $[Sb_2Se_3]/([GeSe_2]+[Sb_2Se_3])$ , i.e.  $m = y/(x+y)$ , are presented in Figs. 5-9.

#### 4. Discussion

As can be seen in Fig. 5, when  $m$  grows (at  $z=10$  and 30 mol. % PbTe)  $T_g$  passes across a weakly expressed maximum at about  $m \approx 0.2$ . It is interesting to note that for the compositions that do not contain PbTe ( $z=0$ ),  $T_g$  for the binary  $GeSe_2$ - $Sb_2Se_3$  ChGs decreases in the whole concentration range when  $m$  varies from 0.0 to 0.6 [15]. This means that the maximum in the dependence  $T_g(m)$  is a characteristic feature for the PbTe containing glasses. Furthermore, it should be noted that  $T_g$  decreases with increase of the PbTe content (for  $m=const$ ).

It is rather difficult to predict the  $T_g$  variation because of the influence of many factors:

(i) On the one hand the melting temperature of  $Sb_2Se_3$  is lower than that of the  $GeSe_2$  glass-former, while those of PbTe is higher, but the ratio between this components does not effect regularly on the  $T_g$  values. The PbTe compound is not obtained in glassy state and its introduction should lead to decrease of  $T_g$ ; (ii) The  $Sb_2Se_3$  compound is a very good modifier [14,20] and improves the  $GeSe_2$  glass-forming ability which increase the solubility of the third component, in this case PbTe, in the  $GeSe_2$ - $Sb_2Se_3$  couple (see Fig. 3). Besides of this, the addition of  $Sb_2Se_3$  to the glassy alloys will decrease  $T_g$  similarly to the PbTe influence; (iii) In addition, taking into account that Pb is an analogue to Ge it could be expected that Pb will substitute Ge in the glassy structure, while Te will replace Se according to the same considerations. As a result, these substitutions will favor the glass formation and  $T_g$  will increase; (iv) Moreover, due to its linear molecule PbTe can be incorporated in the linear chains  $-Se-Ge-Se-Sb-Se-$  of the  $(GeSe_2)_x(Sb_2Se_3)_{1-x}$  glasses cross-linking these linear structural units. This additional structural netting will increase  $T_g$ .

The course of the dependence  $T_g(z)$  is a result of the simultaneous effect of the above factors, as at  $m > 0.2$  the first two are predominant, while at  $0.0 \leq m \leq 0.2$  more determinant are the last two.

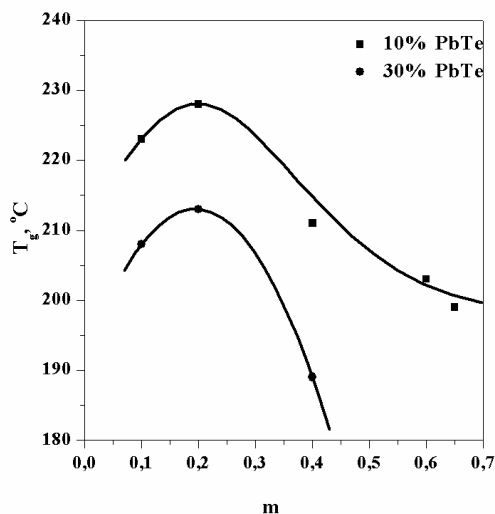


Fig. 5. Dependence of  $T_g$  on the composition of the investigated ChGs.

The compositional dependences of  $T_{cr}$  and  $T_m$  are impeded by the sophisticated composition of the investigated ChGs. Due to the multicomponent character, crystallization of two phases was registered in more of the compositions. In spite of that, certain regularity in the effect of the PbTe content at  $m=const$  and  $Sb_2Se_3/GeSe_2$  ratio at  $z=const$  on  $T_{cr}$  and  $T_m$  was observed. It should be noted that not in all compositions a second phase crystallizes because that is why our further considerations will be focused on the arbitrary higher  $T_{cr}$  and lower  $T_m$  (Table 2). The characteristic temperatures  $T_{cr}$  and  $T_m$  decrease when  $Sb_2Se_3$  content (at constant PbTe content) and PbTe content (at  $(Sb_2Se_3)/(GeSe_2+Sb_2Se_3)=const$ ) increase (Figs. 6 and 7), which should be expected as the introduction of  $Sb_2Se_3$  and/or PbTe generally lead to a decrease of the stability of the ChGs against crystallization.

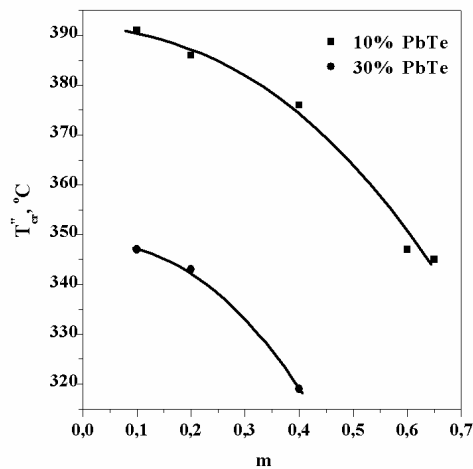


Fig. 6. Dependence of  $T_{cr}$  on the composition of the investigated ChGs.

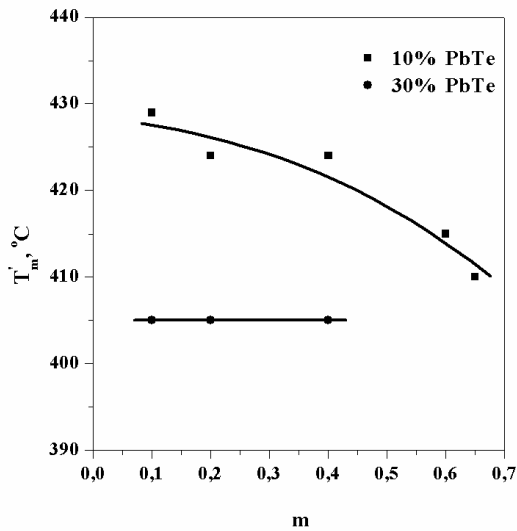


Fig. 7. Dependence of  $T_m$  on the composition of the investigated ChGs.

The studies of the phase diagrams of the binary Ge-Se [21,22],  $\text{GeSe}_2\text{-PbTe}$  [23] and  $\text{GeSe}_2\text{-Sb}_2\text{Se}_3$  [24] systems reveal the presence of eutectics which a prerequisite for the existence of large glass-forming region in the ternary  $\text{GeSe}_2\text{-Sb}_2\text{Se}_3\text{-PbTe}$  system. On the other hand, it should be expected stronger compositional influence on  $T_m$  values, which is confirmed by the experimental results obtained (Fig. 7). The existence of eutectic equilibria in the related  $\text{GeSe}_2$ -based binary systems is indicative for the existence of ternary eutectics in the examined pseudo-ternary system, in which the glass-formation is much more favorable from the enhanced number of the structural units. This is verified by the relatively high values of the Hruby's criterion  $K_G$ , which gives information about the glass formation ability in a definite concentration zone of the system (Fig. 8).

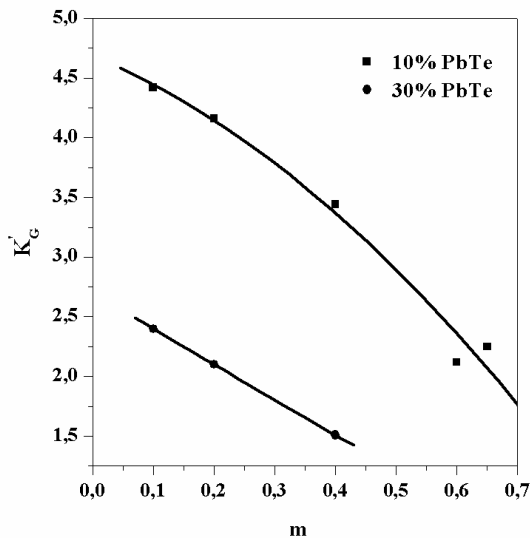


Fig. 8. Dependence of  $K_G$  on the composition of the investigated ChGs.

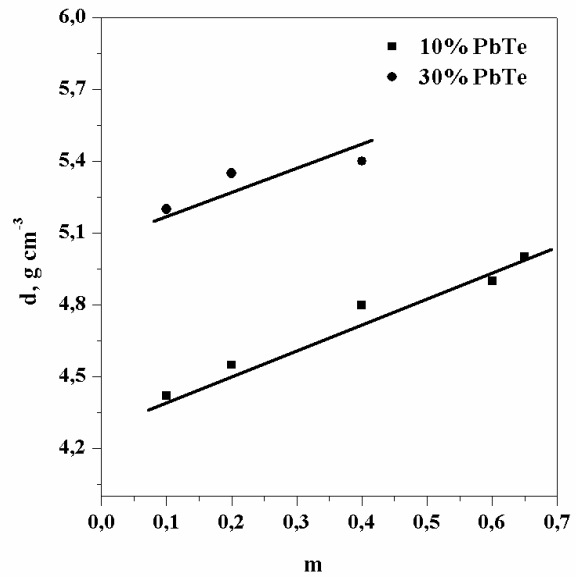


Fig. 9. Dependence of  $d$  on the composition of the investigated ChGs.

The density increases with the  $\text{Sb}_2\text{Se}_3$  and/or  $\text{PbTe}$  percentage elevation, as the dependences  $d(m)$  at  $z=10$  and  $z=30$  mol %  $\text{PbTe}$  are located almost in parallel (Fig. 9).

The compactness  $C$  as a criterion for the densification or looseness of the glassy network varies in very narrow limits in dependence of the  $\text{Sb}_2\text{Se}_3$  and/or  $\text{PbTe}$  concentrations. The  $C$  values for the investigated glasses are very close to zero which is indicative that both  $\text{Sb}_2\text{Se}_3$ , and  $\text{PbTe}$  are optimally embed in the primary glassy matrix built of  $\text{GeSe}_{4/2}$ -tetrahedra. In stoichiometric aspect the embedment of the  $\text{SbSe}_{3/2}$  pyramids in the glassy network composed of  $\text{GeSe}_{4/2}$  tetrahedral units will promote cross-linking of the layers. Meanwhile, the network is partially broken because of the fact that  $\text{Sb}$ -atoms connect three  $\text{Se}$ -atoms which simultaneously participate in the  $\text{SbSe}_{3/2}$  pyramids and  $\text{GeSe}_{4/2}$ -tetrahedra with their two-valence bonds; they are bonded to  $\text{Sb}$  by one of their two bonds and by the other participate in the  $\text{GeSe}_{4/2}$ -tetrahedra. In that way, one of the bonds of the four  $\text{Se}$ -atoms connected to  $\text{Ge}$  remains free. The  $\text{Sb}_2\text{Se}_3$  addition to the  $\text{GeSe}_2$ -based glasses influences the glass compactness in two opposite directions: the ability of the  $\text{SbSe}_{3/2}$  pyramids to cross-link the  $\text{GeSe}_{4/2}$ -glassy structure should lead to increase of  $C$ , while the breaking of the  $\text{GeSe}_{4/2}$ -tetrahedral matrix will stimulate the occurrence of voids, which leads to decrease of  $C$ . These two opposite trends determine the course of the  $C(m)$  dependence at  $z=\text{const}$ , as a result of which  $C$  varies in very narrow limits. It is logically to expect that, the increase of the  $\text{PbTe}$  content at a constant  $\text{Sb}_2\text{Se}_3/\text{GeSe}_2+\text{Sb}_2\text{Se}_3$  ratio will increase the structural compaction, because  $\text{Ge}$  and  $\text{Se}$  in the  $\text{GeSe}_2$ -glassy structure will be replaced by their analogs  $\text{Pb}$ - and  $\text{Te}$ - atoms, respectively, which possess smaller atomic radii.

## 5. Conclusions

New chalcogenide glasses from the GeSe<sub>2</sub>-Sb<sub>2</sub>Se<sub>3</sub>-PbTe system were synthesized and the glass-forming region was determined. It is situated in the GeSe<sub>2</sub>-rich part and lies partially on the GeSe<sub>2</sub>-Sb<sub>2</sub>Se<sub>3</sub> (0-70 mol % Sb<sub>2</sub>Se<sub>3</sub>) and GeSe<sub>2</sub>-PbTe (15.0-57.5 mol % PbTe) sides in Gibb's concentration diagram. No glass-formation was observed in the binary Sb<sub>2</sub>Se<sub>3</sub>-PbTe system. The synthesized glasses were investigated with respect to their phase transformations temperatures (T<sub>g</sub>, T<sub>cr</sub> and T<sub>m</sub>) and density (d). The compactness (C) and Hruby's criterion (K<sub>G</sub>) were calculated from the experimental data obtained. Relationships between the investigated properties and the glass composition were established and discussed in terms of structural considerations.

## Acknowledgments

The authors acknowledge gratefully the financial support for this work from the Ministry of Education and Science (Science Researches Fund – contract DO 02-123).

## References

- [1] E. Bychkov, D. L. Price, C. J. Benmore, A. C. Hannon, *Solid State Ionics* **154-155**, 349 (2002).
- [2] F. Smektala, C. Quemard, L. Leneindre, J. Lucas, A. Barthélémy, C. De Angelis, *J. Non-Cryst. Sol.* **239**, 139 (1998).
- [3] V. K. Tikhomirov, *J. Non-Cryst. Sol.* **256-257**, 328 (1999).
- [4] A. S. Soltan, A. H. Moharram, *Physica B* **349**, 92 (2004).
- [5] A. Zakery, S. R. Elliot, *J. Non-Cryst. Sol.* **330**, 1 (2003).
- [6] B. Bureau, X. H. Zhang, F. Smektala, J.-L. Adam, J. Troles, H.-li Ma, C. Boussard-Pledel, J. Lucas, P. Lucas, D. Le Coq, M. R. Riley, J.H. Simmons, *J. Non-Cryst. Sol.* **345-346**, 276 (2004).
- [7] V. Vassilev, K. Tomova, S. Boycheva, *J. Non-Cryst. Solids* **353**, 2779 (2007).
- [8] V. Vassilev, S. Hadjinikolova, S. Boycheva, *Sens. Actuators B* **106**, 401 (2005).
- [9] J. Schubert, M. Schoning, C. Schmidt, M. Siegert, St. Mesters, W. Zander, P. Kordus, H. Luth, A. Legin, Yu. G. Mourzina, B. Seleznev, Yu. G. Vlasov, *Appl. Phys. A* **69**, S803 (1999).
- [10] Yu. Vlasov, Y. Ermolenko, A. Legin, Yu. Mourzina, *J. Anal. Chem.* **54**, 476 (1999).
- [11] A. Pradel, O. Walls, C. Cali, G. Taillades, A. Bratov, C. Dominguez, M. Ribes, *J. Optoelectron. Adv. Mater.* **3**, 641 (2001).
- [12] S. Marian, D. Tsiulyanu, H.-D. Liess, *Sens. Actuators B* **78**, 191 (2001).
- [13] P. Boolchand, D. G. Georgiev, M. Micolaut, *J. Optoelectron. Adv. Mater.* **4**, 823 (2002).
- [14] S. Boycheva, V. Vassilev, P. Petkov, *J. Optoelectron. Adv. Mater.* **3**, 503 (2001).
- [15] V. Vassilev, S. Boycheva, Z. G. Ivanova, *J. Mater. Sci. Letters* **17**, 2007 (1998).
- [16] V. Vassilev, K. Tomova, V. Parvanova, S. Boycheva, *J. Alloys Compd.*, <http://dx.doi.org/10.1016/j.jallcom.2009.06.029>, in press.
- [17] Joint Committee on Powder Diffraction Standards-International Center for Diffraction Data PDF 42-104.
- [18] Joint Committee on Powder Diffraction Standards-International Center for Diffraction Data PDF 15-861.
- [19] Joint Committee on Powder Diffraction Standards-International Center for Diffraction Data PDF 40-0893.
- [20] S. Boycheva, V. Vassilev, Z. Ivanova, *J. Phys. D: Appl. Phys.* **32**, 529 (1999).
- [21] S. Karbanov, E. Statnova, V. Zlomanov, A. Novoselova, *J. Nation. Mosc. Uni., ser. 2, Chemistry* **13**, 531 (1972) (in Russian).
- [22] L. Ross, M. Bourgon, *Canad. J. Chem.* **47**, 2555 (1969).
- [23] V. Vassilev, K. Tomova, S. Parvanov, *Thermochim. Acta* **459**, 12 (2007).
- [24] G. Orlova, I. Kozhina, V. Korolenko, *J. Leningr. Uni.* **4**, 90 (1973).

\*Corresponding author : [venciv@uctm.edu](mailto:venciv@uctm.edu)